Fracture Mechanics of Concrete and Concrete Structures -
Assessment, Durability, Monitoring and Retrofitting of Concrete Structures- B. H. Oh, et al. (eds)

An experimental study on the effects of cracks on corrosion distribution and bond behavior of reinforcing bar

K. Kobayashi & K. Rokugo
Gifu University, Gifu, Japan

K. Sugiki
JR Tokai Construction, Nagoya, Japan

T. Inaguma
JR Central Consultants, Nagoya, Japan

S. Maruyama
Central Japan Railway Company, Nagoya, Japan

ABSTRACT: In this study, the effects of cover concrete cracks on corrosion distribution along the rebar and on the bond behavior of corroded rebar were investigated using tension specimens with rebar corroded either by a chloride spray or electrolytic corrosion. The following were examined: the relationship between the corrosion length and bondless length, the effect of tension cracks on the localization of corrosion, and the effects of cracks and corrosion on the bond energy and the tensile rigidity.

1 INTRODUCTION

Reinforced concrete is intrinsically a durable composite material. However, when the passive film on the steel surface is destroyed by the chloride of marine salt or of de-icing salt, the steel corrodes and the reinforcing concrete structure deteriorates. Since the volume of corrosion products is several times larger than that of sound steel, the rebar corrosion causes a high expansive pressure, which leads to formation of cracks in the cover concrete. This facilitates chloride penetration into the cover concrete, accelerating the corrosion progress.

Using high-performance concrete and giving a large cover depth can prevent chloride from reaching the rebar surface. On the other hand, RC structures are designed to tolerate bending cracks, and chloride can reach the rebar through these cracks. Uneven distribution of chloride along the rebar causes formation of a macro-cell corrosion circuit, resulting in locally severe corrosion.

In assessing the residual performance of an RC member suffering steel corrosion, it is important to consider how much the bonding properties have deteriorated. Corrosion on the rebar at an early stage increases the bond strength due to expansive pressure. However, once cracks are formed in the cover concrete, the bond strength is reduced. The integrity between the rebar and concrete is then lost, and so is the plane conservation. Numerous researches have been conducted on laboratory test specimens to confirm the effect of corrosion that enhaces the bonding properties. However, it is also important to clarify the effect of uneven corrosion distribution on the bonding properties, because RC members often suffer load-induced cracks as mentioned above.

Therefore, in this study, the bond behavior of corroded steel was investigated through a tension test using tension specimens with rebars corroded by both chloride spraying and electrolytic corrosion. The effect of cover concrete cracks on the corrosion distribution on the rebar was also investigated.

2 EXPERIMENTAL PROCEDURE

2.1 *Specimen*

Figure 1 illustrates the dimensions of the tension specimen. Tables 1 and 2 are the lists of specimens. Three test pieces were prepared for each type of specimens. All the specimens had a cross-section of 100 x 100mm, and a length of 1000mm. For rebar, a screw-reinforcing bar D16 was used. Ready-mixed concrete with a nominal compressive strength of 21MPa, a slump of 8cm, a maximum size of coarse aggregate of 20mm was used.

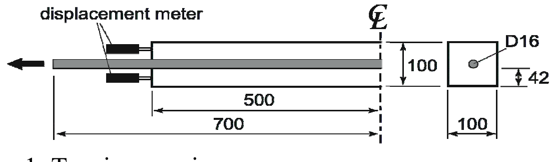

Figure 1. Tension specimen.

Table 1. Chloride-induced corrosion specimens.

	Crack width	Deterioration period
0-L-N	-	180days
0.1-S-N	0.1mm	60days
0.1-L-N		180days
0.2-S-N	0.2mm	60days
0.2-L-N		180days
0.4-S-N	0.4mm	60days
0.4-L-N		180days

Table 2. Electrolytic corrosion specimens.

	Corrosion loss	Crack width
0-0-N	-	-
0.2-2-N	2%	0.2mm
0-2-N		-
0.2-5-N	5%	0.2mm
0-5-N		-
0.2-10-N	10%	0.2mm
0-10-N		-

2.2 *Tension test (before corrosion)*

A tension test was carried out using a hydraulic jack only to the specimens having a crack width of from 0.1 to 0.4mm as shown in Tables 1 and 2. The load was measured by a load cell. The displacement at both ends of concrete was measured using four high-sensitive displacement meters, two each at both ends (see Fig. 1) to determine an elongation of the entire concrete part. After the specimens were unloaded, surface cracks were measured with a digital measuring instrument to obtain an average width of residual cracks.

2.3 *Acceleration of corrosion*

On the chloride-induced corrosion specimens, a 3% sodium chloride solution was sprayed for five minutes every 6 hours throughout the respective periods shown in Table 1. The solution in the system was replaced every 720 hours to keep the solution density constant, and the positions of specimens in the spray chamber were rotated.

Figure 2 illustrates the electrolytic corrosion method used in this experiment. The electrolyte used was a 3% sodium chloride solution. A corrosion circuit was made up of a constant-current power supply, an anode of rebar, and a cathode of copper plate set beneath the specimen. The current magnitude was set to be 0.45A per specimen (0.865mA/cm^2, per unit surface area of rebar). Corrosion acceleration time was calculated using Equation 1 (Tamori et al. 1988) to obtain the corrosion loss shown in Table 2.

$$\Delta W = 0.766 \times i \times t \tag{1}$$

where;

ΔW : Corrosion loss (g)

i: current (A)

t: time (hour)

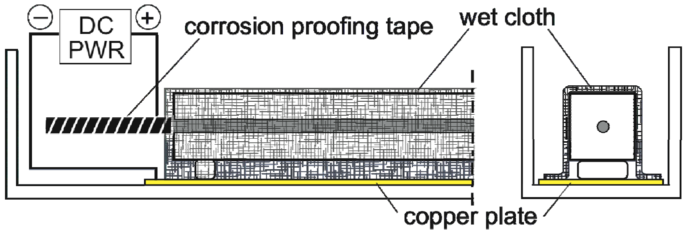

Figure 2. Electrolytic corrosion.

2.4 *Tension test (after corrosion)*

The tension test was carried out in the same manner as described in section 2.2. Pi displacement transducers were set such as to bridge across tension cracks that were introduced by the tension test carried out before corrosion to measure changes in the crack opening during the loading. For the specimens without any tension cracks, 10 pi displacement transducers were arranged closely together on the concrete surface to measure changes in the crack opening.

2.5 *Investigation of corrosion state*

The rebar was taken out from each specimen after the tension test. Following a JCI method (JCI 1987), the rebar was immersed in a solution of 10% diammonium hydrogen citrate for 24 hours to remove rust. The rust that could not be removed by the immersion was chipped off by a pick. Corrosion loss was then calculated from the measured weight of cleaned rebar.

Furthermore, the surface profile of corroded rebar was measured by a three dimensional laser scanner (3D scanner), at intervals of 0.2mm in a longitudinal direction and 0.18^{o} in a circumference direction. The length of the target region was 100mm.

3 CHLORIDE-INDUCED CORROSION

3.1 *Outline of corrosion state*

Chloride spraying for half a year caused only a slight corrosion. It was observed only within cracked areas, and the cross-sectional loss was negligible. No corrosion crack was observed on the cover concrete.

As mentioned in the previous chapter, the surface profile of steel was measured after the tension test. Therefore, the effect of plastic deformation of rebar cannot be eliminated completely from the results of the surface profile measurement. It is therefore very difficult to determine whether the cross-sectional loss was caused actually by corrosion or by the plastic deformation with regard to the test pieces that were only slightly corroded. Here, the corrosion length measured by a vernier caliper was employed as an index of corrosion level for the specimens deteriorated by chloride-induced corrosion. Figure 3 shows the relationship between corrosion length and the width of tension cracks on the cover concrete.

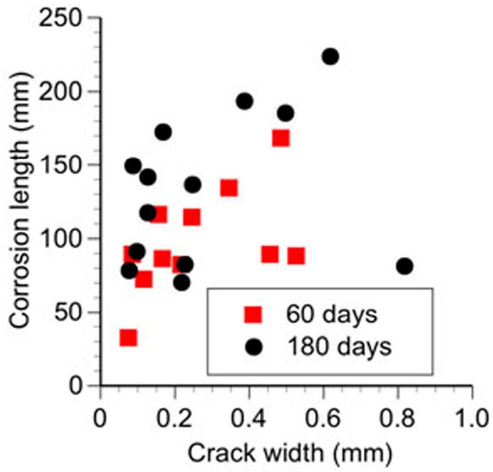

Figure 3. Relationship between the corrosion length and the width of tension crack.

Chloride penetrates into concrete through cracks, and goes further into the longitudinal direction through the weak interfacial zone between the rebar and concrete, resulting in corrosion on the steel surface around the crack. In this study, since the rebar had been yielded to form residual tensile cracks, bond fracture occurred at the interface between the rebar and concrete. As chloride penetrates through the fractured part, the length of corrosion is affected by the state of bond. This is considered to be the reason for the increase in corrosion length with the increase incrack width and corrosion acceleration period as shown in Figure 3.

3.2 *Tension test*

Figure 4 shows examples of the load-strain curves of the specimens obtained from the results of the two tension tests: One was carried out before corrosion to introduce cracks into specimens, the other after corrosion induced by spraying a chloride solution for 180 days.

With some specimens, the slope of the loading curve after corrosion was slightly larger than that of the unloading curve before corrosion. In these specimens, there were no corrosion cracks in the cover concrete. Therefore, the corrosion progress is considered to have enhanced the bond because of the expansive pressure. However, with most specimens, there was no change in the slope of the loading curve even after the chloride spraying for 180 days. Accordingly, it is considered that a slight corrosion as discussed here hardly affects the bonding properties of deformed rebar.

3.3 *Bondless length*

As described above, the bondless length is considered to affect the corrosion distribution. In this section, the bondless length is further discussed. Since the cover concrete had not suffered any corrosion cracks during the corrosion acceleration period in which chloride was sprayed for 180 days, it was assumed that the length of bondless regions that had been formed by the first tension test around the tension cracks did not increase during the corrosion acceleration period. Based on this assumption, the bondless length was calculated using Equation 2 from the results of the second tension test that was carried out after the corrosion acceleration period. For the calculation, a common load of 40kN and its corresponding crack width, measured by the pi displacement transducers, were used. The bondless length thus calculated was almost constant before the point where the specimen yielded in the second tension test.

$$L = \frac{AE\omega}{P} \tag{2}$$

where;

L: Bondless length (mm)
A: Nominal cross-sectional area of rebar (mm^2)
E: Young's modulus of rebar (kN/mm^2)
P: Load (kN, =40kN)

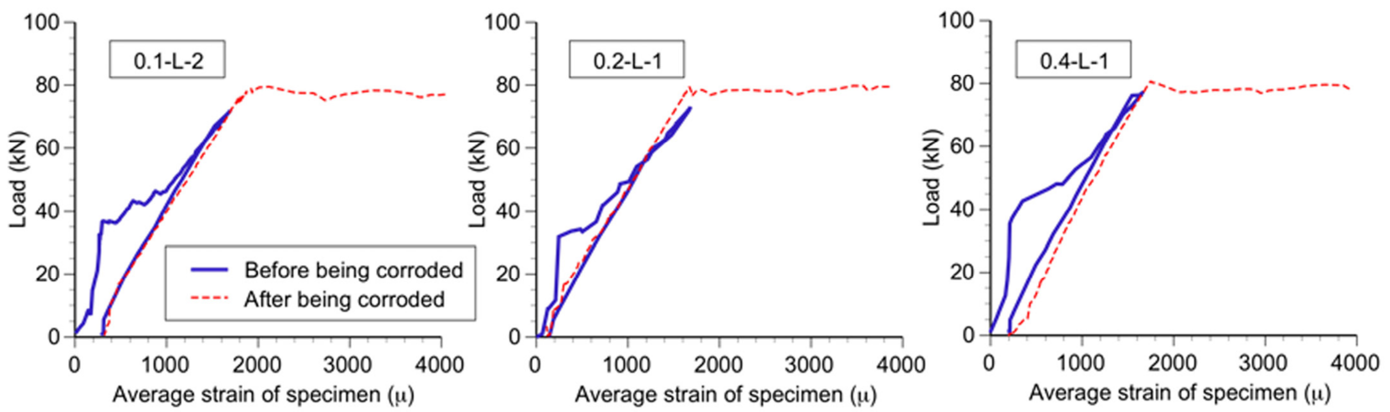

Figure 4. Results of the tension test of specimens on which chloride solution was sprayed for 180 days.

ω: Crack width by pi displacement transducer (mm, corresponding to a load of 40kN)

Figure 5 shows the relationship between the bondless length and the corrosion length on the rebar. The corrosion length becomes smaller than the bondless length after 60 days of chloride spraying, while the corrosion length becomes larger than the bondless length after 180 days of chloride spraying. This is because of enlargement of corroded area through penetration of chloride into the bond fracture region or the interfacial zone between the rebar and concrete.

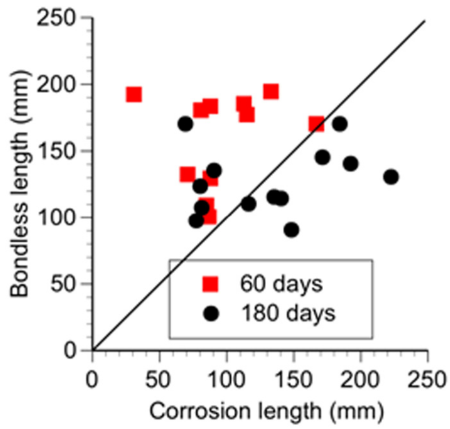

Figure 5. Relationship between bondless length and corrosion length.

The above results made it clear that corrosion would progress from cracks as time passes. However, the specimens that had been sprayed with chloride suffered only slightly and the bond behavior was barely affected. The following chapter will discuss the effect of corrosion on the bond properties based on the results obtained using the electrolytic corrosion method, which is more controllable and can accelerate corrosion much faster.

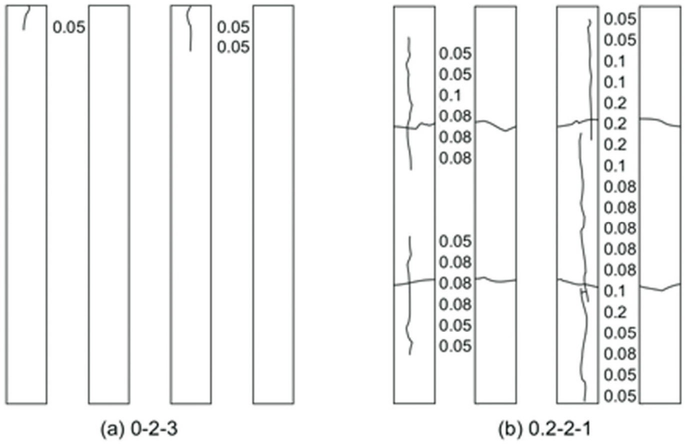

Figure 6. Examples of corrosion crack distribution on cover concrete.

4 ELECTROLYTIC CORROSION

4.1 *Outline of corrosion state*

Figure 6 illustrates examples of crack distributions on the cover concrete that was deteriorated by electrolytic corrosion. All the specimens corroded by the electrolytic corrosion method had corrosion cracks on the cover concrete along the rebar. Furthermore, the specimens to which tension crack(s) had been introduced before corrosion had longer cracks than those without tension cracks. In addition, the crack width was larger around the tension crack(s) as shown in Figure 6.

Figure 7 shows examples of the distributions of

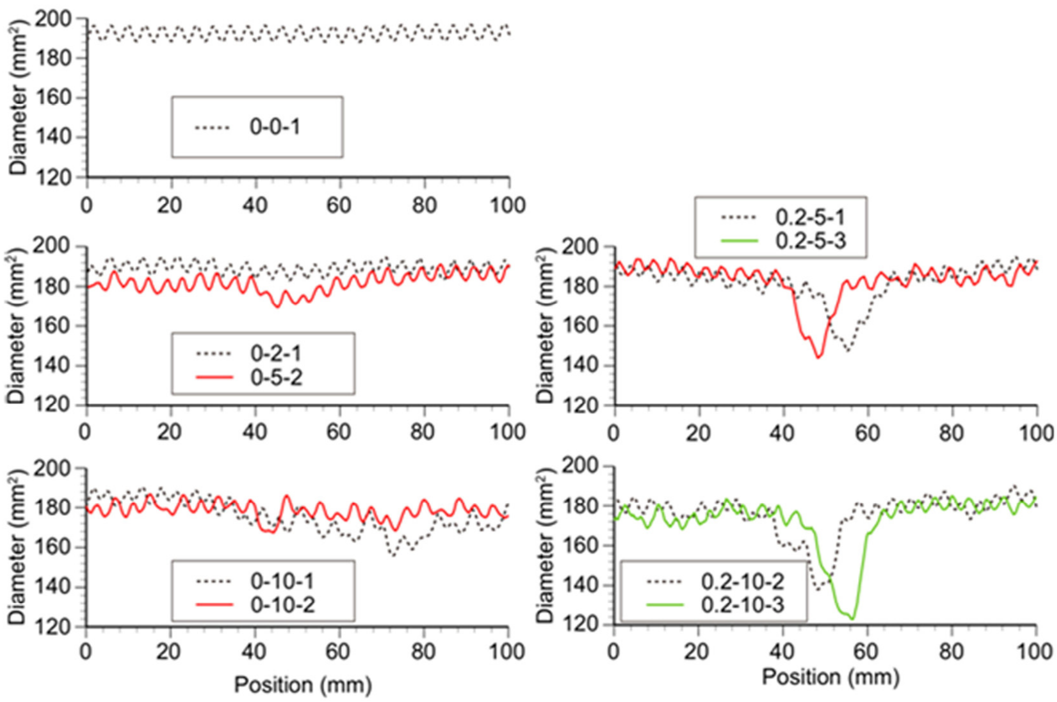

Figure 7. Examples of the distribution of rebar cross-sectional area.

rebar cross-sectional areas measured by a 3D scanner. The specimens without tension cracks lost cross-sectional areas all along the length of rebar with some dispersion in distribution. On the other hand, the specimens with tension cracks lost cross-sectional areas of rebar more remarkably around the tension crack. The intense corrosion progress in this region apparently caused a higher expansive pressure, resulting in the larger crack width around the tension crack(s) (see Fig. 6)

4.2 *Tension test*

4.2.1 *Specimen without tension crack*

Figure 8 shows examples of the load-strain curves of corroded specimens to which tension cracks had not been introduced before corrosion. It is clear form this figure that the specimen with a targeted corrosion loss of 10% suffered a large decline in tensile strength. However, there is apparently no clear impact of rebar corrosion on the bonding properties. Next, the average tensile strain of concrete was calculated using Equation 3 (Maekawa & Okamura 1991, Matsuo et al. 2001) from the results of the tension test (see Fig. 9).

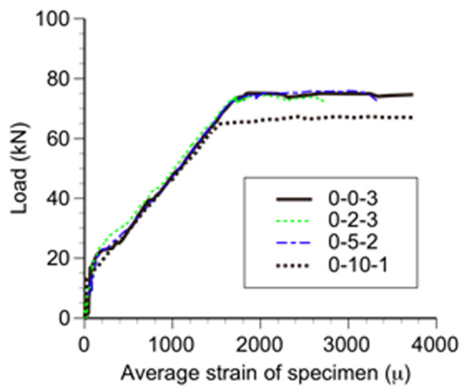

Figure 8. Examples of the load-strain curves of corroded specimens to which tension crack(s) had not been introduced before corrosion.

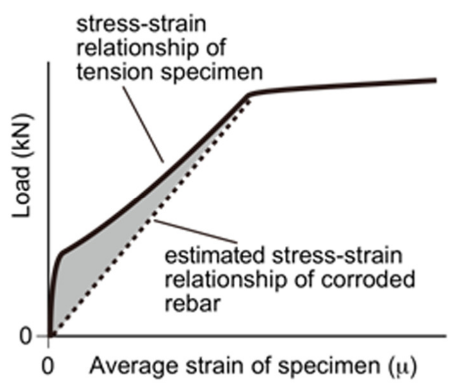

Figure 9. Calculation of the average tensile strain of concrete.

$$\sigma_{c,av} = \frac{P - A_{s,av} E_s \varepsilon_{av}}{A_c} \qquad (3)$$

where,

$\sigma_{c,av}$: Average strain of concrete

P: Load (N)

$A_{s,av}$: Average cross-sectional area of rebar

E_s: Young's modulus of rebar

ε_{av}: Average strain of rebar under concrete cover (=Average strain of concrete)

A_c: Cross-sectional area of concrete

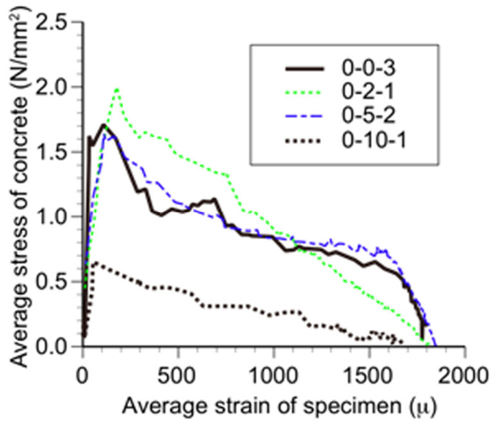

Figure 10. Average tensile strain of concrete.

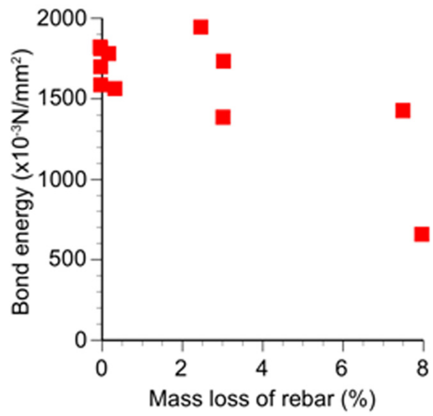

Figure 11. Relationship between the corrosion loss and the bond energy.

Figure 10 shows examples of the calculated tensile stress-strain curves of concrete. The areas surrounded by these curves were calculated and defined as "bond energy". Figure 11 shows the relationship between the corrosion loss and the bond energy. According to these figures, the tensile stress of concrete and the bond energy do not change when the corrosion loss was within several percent, while they start to decline after the corrosion loss exceeds 8%. With deformed bar, mechanical interlocking of transverse ribs plays a much greater role in the rebar bond than adhesion between the steel surface and concrete. This is considered to be the reason why the rebar corrosion did not affect the bonding properties until the corrosion loss reached 8%.

4.2.2 *Specimen with tension crack*

Figure 12 shows examples of the load-strain curves of corroded specimens to which tension crack(s) had been introduced before being corroded by the electrolytic corrosion method. It can be clearly seen that the slope of the loading curve after corrosion was

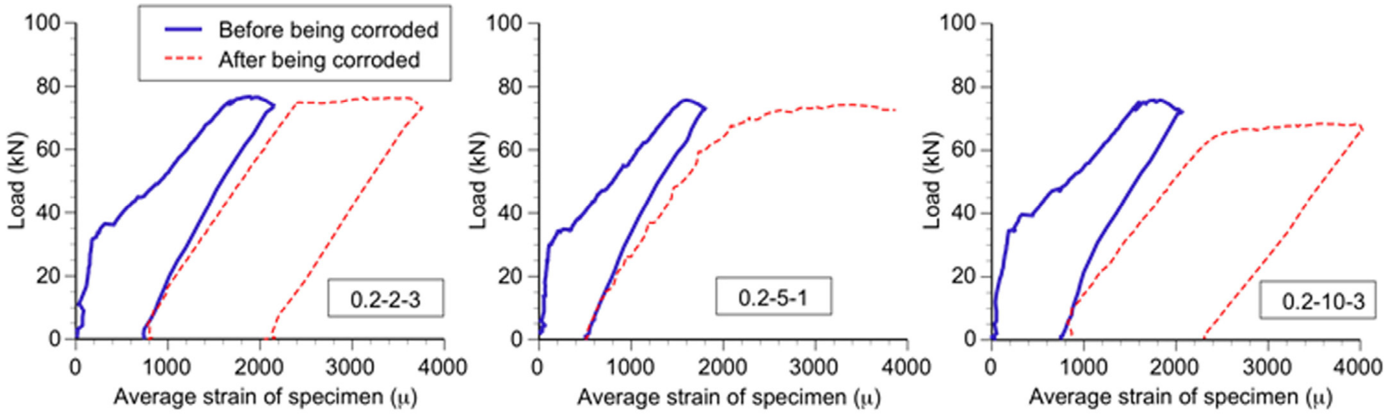

Figure 12. Results of tension test of specimens deteriorated by electrolytic corrosion.

smaller than that of the unloading curve before corrosion, unlike the specimens corroded by chloride spraying. The specimens that had contained tension crack(s) before corrosion suffered longer and wider cover cracks due to rebar corrosion, as shown in Figure 6, and their bond had declined. In addition, these specimens had suffered more localized cross-sectional loss as shown in Figure 7, because of which the apparent Young's modulus of rebar had also declined, which in turn led to the decline of sectional rigidity. As shown in Figure 13, the sectional rigidity of tension specimens declines with an increase in the loss of cross-sectional area.

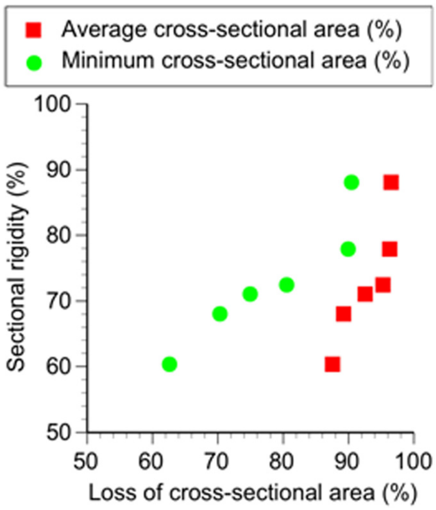

Figure 13. Relationship between the cross-sectional area loss and the sectional rigidity of tension specimen.

5 CONCLUSIONS

In this study, tension specimens were prepared, which were sprayed with chloride solution or underwent an electrolytic process to induce corrosion. The chloride solution was sprayed on the specimen for 6 months. The target amount of corrosion loss by the electrolytic corrosion was set to be 2 to 10%. Tension tests were carried out both before and after the corrosion to investigate the effect of corrosion on the bonding properties of rebar. Furthermore, the effect of tension cracks on the corrosion distribution was investigated using a 3D scanner.

The results on the chloride-induced corrosion can be summarized as follows:

- In some of the specimens to which tension crack(s) had been introduced, the bonding properties improved due to the corrosion before the generation of corrosion cracks, ;
- While no clear correlation was observed between the tension crack width and the bondless length, the corrosion length grew longer than the bondless length as time passed.

The results on electrolytic corrosion can be summarized as follows:

- Tension cracks fomented the generation of corrosion cracks along the rebar.
- Tension cracks made the rebar corrosion around the cracks even more localized.
- Bond energy did not decline while the corrosion loss was within several percent; it started to decline after the corrosion loss reached 8%.
- The sectional rigidity of tension specimens declined with an increase in the loss of cross-sectional area, due to the localized cross-sectional loss of rebar.

REFERENCES

JCI-SC1. 1987. Corrosion evaluation method of steel materials in concrete (in Japanese).

Maekawa, K., & Okamura, H. 1991. Nonlinear Analysis and Constitutive Models of Reinforced Concrete, Gihodo, Japan.

Matsuo H., Gokaku W. and Shimomura T., 2001, Tension Stiffness of Reinforced Concrete Member with Corroded Reinforcement, Proceeding of JCI, 23(3), pp. 1327-1332 (in Japanese).

Tamori, K., Maruyama, K., Odagawa, M. and Hashimoto, C. 1988. Cracking behavior of reinforced concrete members due to corrosion of reinforcement. Proceedings of JCI, 10(2), pp.505-510 (in Japanese).